JACS
JOURNAL OF THE AMERICAN CHEMICAL SOCIETY
Communication
pubs.acs.org/JACS

# Photoluminescent Gold–Copper Nanoparticle Alloys with Composition-Tunable Near-Infrared Emission

Christopher M. Andolina, Andrew C. Dewar, Ashley M. Smith, Lauren E. Marbella, Michael J. Hartmann, and Jill E. Millstone*

Department of Chemistry, University of Pittsburgh, Pittsburgh, Pennsylvania 15260, United States

Supporting Information

**ABSTRACT:** Discrete gold nanoparticles with diameters between 2 and 3 nm show remarkable properties including enhanced catalytic behavior and photoluminescence. However, tunability of these properties is limited by the tight size range within which they are observed. Here, we report the synthesis of discrete, bimetallic gold–copper nanoparticle alloys (diameter ≅ 2–3 nm) which display photoluminescent properties that can be tuned by changing the alloy composition. Electron microscopy, X-ray photoelectron spectroscopy, inductively coupled plasma mass spectrometry, and pulsed-field gradient stimulated echo $^1$H NMR measurements show that the nanoparticles are homogeneous, discrete, and crystalline. Upon varying the composition of the nanoparticles from 0% to 100% molar ratio copper, the photoluminescence maxima shift from 947 to 1067 nm, with excitation at 360 nm. The resulting particles exhibit brightness values (molar extinction coefficient ($\varepsilon$) × quantum yield ($\Phi$)) that are more than an order of magnitude larger than the brightest near-infrared-emitting lanthanide complexes and small-molecule probes evaluated under similar conditions.

It has been known for centuries that alloyed materials can dramatically enhance the properties of their constituent metals and, like their monometallic counterparts, may also exhibit significant changes in their physical properties at the nanometer length scale.[1] One particularly interesting class of these materials is small metal nanoparticles (diameter $d$ ≅ 2–5 nm) which exhibit properties different from both metal clusters (< 200 atoms) and larger metal nanomaterials ($d$ > 5 nm).[2] These "few nm" particles display unique catalytic and optoelectronic behaviors. For example, gold, silver, and copper nanoparticles all exhibit photoluminescence (PL).[2,3] Gold nanoparticles (AuNPs) exhibit PL emission throughout the visible and into the near-infrared (NIR) depending upon their size, shape, and surface chemistry.[2−8] Yet, aspects of the PL from metallic nanostructures are not well understood and proposed mechanisms differ for AuNPs that exhibit localized surface plasmon resonances (LSPRs) and small AuNPs that do not.[2,3]

In anisotropic NPs that exhibit LSPRs, PL is observed between ∼630 and 750 nm[4,9,10] and is attributed to emission from the plasmon band.[2−4] As the diameter of the NP decreases below 3 nm, the LSPR of the AuNPs is no longer discernible, and instead these particles exhibit PL in the NIR region with a large shift (∼600 nm) between their absorption and emission wavelengths.[7,5,11] Further decreases in particle size result in a hypsochromic shift of the NIR emission and an increase in quantum yield ($\Phi$).[2,3,12,13] PL from these small AuNPs is attributed to emission from surface states, since experiments have shown that the number of gold(I)–thiolate bonds on the particle surface is well-correlated with observed PL intensity.[8,12,13] Because NIR PL from AuNPs occurs only at small diameters, the ability to tune this optoelectronic behavior has been limited.[2,3,5,12] However, tuning of the particle composition within the same size range could allow for increased versatility in this class of nanomaterials and present a new perspective on the underlying PL phenomena of small metal NPs.

Here, we describe the synthesis of small, discrete gold–copper NP alloys with tunable compositions from 0 to 100% molar ratio Cu ($d$ ≅ 2–3 nm). The resulting materials display some of the first observations of composition-driven, tunable PL in the NIR region. To synthesize these nanoalloys, we hypothesized that the molar ratio of metal precursors may be adjusted in order to mediate the final metal molar ratio in the resulting NP. However, obtaining tunable alloy composition over a wide range of molar ratios may be synthetically challenging due to metal phase separation[14,15] and limitations described by Hume-Rothery[16] (although several nanocrystalline intermetallic materials have been successfully prepared).[1,17−19]

In a typical experiment, alloyed NPs were prepared in aqueous solution under ambient conditions by co-reduction of $HAuCl_4$ and $Cu(NO_3)_2$ in the presence of poly(ethylene glycol) methyl ether thiol (PEG-SH, average $M_n$ = 1000 Da) using $NaBH_4$ (Table S1, complete details in the Supporting Information (SI)). Although PL has been observed from clusters such as $Au_{85}Ag_{55}$[11,12] and $Ag_7Au_6$,[20] we have focused on CuNP alloys in order to avoid any ambiguity from photoreactivity of Ag species (although our synthetic strategy can be used to produce $Au_xAg_y$ alloys (Figure S1), and $Au_xAg_y$ cluster species have been successfully studied previously).[11,21,22] Here, the initial molar ratio of Au to Cu was adjusted from 0% to 100% Cu while holding all other reagent concentrations constant. Particles were purified by centrifugation using molecular weight cutoff filters to remove excess reagents and reaction byproducts. Table 1 summarizes the physical and spectral properties of the NP alloys.

**Received:** January 17, 2013
**Published:** April 2, 2013





dx.doi.org/10.1021/ja400569u | J. Am. Chem. Soc. 2013, 135, 5266–5269

**Table 1. Size, Composition, and Photoluminescence Analysis of $Au_xCu_y$ NPs[a]**

| | lattice constant (Å) | NP composition (% Cu) | | NP size (nm) | | | | | | |
|---|---|---|---|---|---|---|---|---|---|---|
| initial mol % Cu | HRTEM | EDS | ICP-MS | TEM | PFGSE-NMR | $\varepsilon$ at 360 nm ($\times 10^5$ $M^{-1}$ $cm^{-1}$) | $\lambda_{EM}$ (nm) | fwhm (nm) | $\Phi$ ($\times 10^{-4}$) | brightness ($M^{-1}$ $cm^{-1}$) |
| 0 | 3.96 ± 0.12 | 0 | 0 | 2.2 ± 0.5 | 4.7 ± 0.3 | 15.9 | 948 ± 9 | 256 ± 10 | 1.9 ± 0.2 | 302 |
| 20 | 3.99 ± 0.13 | 33 ± 3 | 8 ± 7 | 1.9 ± 0.3 | 5.1 ± 0.8 | 5.08 | 947 ± 4 | 246 ± 4 | 25 ± 4 | 1270 |
| 40 | 3.70 ± 0.08 | 53 ± 5 | 28 ± 8 | 3.0 ± 0.5 | 4.6 ± 0.9 | 19.3 | 966 ± 9 | 250 ± 1 | 17 ± 4 | 3281 |
| 50 | 3.96 ± 0.07 | 48 ± 13 | 39 ± 10 | 3.0 ± 0.8 | 4.6 ± 0.3 | 13.6 | 1004 ± 25 | 253 ± 8 | 8.6 ± 0.3 | 1170 |
| 60 | 3.66 ± 0.13 | 56 ± 14 | 49 ± 12 | 2.6 ± 0.6 | 4.4 ± 0.9 | 10.2 | 1058 ± 8 | 262 ± 16 | 4.6 ± 1.0 | 469 |
| 80 | 3.88 ± 0.16 | 62 ± 8 | 77 ± 8 | 2.8 ± 0.5 | 4.4 ± 0.9 | 8.62 | 1067 ± 7 | 265 ± 17 | 1.9 ± 0.4 | 164 |
| 100 | 4.33 ± 0.10 | 100 | 100 | 2.8 ± 0.9 | 4.8 ± 0.2 | 3.45 | NA | NA | NA | NA |

[a]All values are reported as an average with associated standard deviation (see SI for details of each experiment), unless indicated otherwise. Molar extinction coefficients ($\varepsilon$) and brightness ($\varepsilon \times \Phi$) were calculated from average measured values. NA indicates that the values could not be measured and/or calculated. Standard deviations of the mean are reported for the emission maxima ($\lambda_{em}$), full width at half-maximum (fwhm), and quantum yield ($\Phi$).

The size of the NP alloys was characterized by electron microscopy and pulsed field gradient stimulated echo (PFGSE) $^1$H NMR measurements (Figures 1, S3–S9, and Table 1). The NPs exhibit average diameters of 1.9–3.0 nm for all compositions. Standard deviations of NP diameters were within 15–27% of the average diameter for each alloy composition analyzed (Table 1 and Figure S3). Values obtained from high-resolution transmission electron microscopy (HRTEM) were consistent with the hydrodynamic diameter as determined by $^1$H NMR diffusion measurements which should always be larger than the metallic core diameter. By comparing these measurements, the average thickness of the PEG-SH shell was determined to be 1.6–3.2 nm.

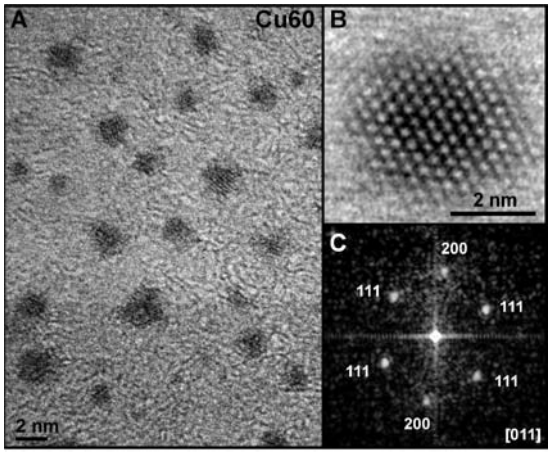


**Figure 1.** (A) HRTEM image of $Au_xCu_y$NPs (40:60 Au:Cu molar ratio) and (B) close-up of a particle lattice with corresponding (C) FFT.

Lattice constants ($a$) calculated from fast Fourier transform (FFT) analysis of HRTEM images show significant deviations from the lattice constant of bulk gold and are consistent with the formation of alloyed nanostructures (Figures 1, S4–S9, and Table 1). Because the lattice constant of Au is larger than that of Cu, we may expect to observe a general decrease in lattice constant as the incorporation of Cu increases. However, this trend does not consider lattice strain that appears at small particle sizes or intermetallic states that are known to deviate from this trend.[23]

X-ray photoelectron spectroscopy (XPS) clarifies whether oxidation has impacted the observed crystal structures. For alloyed compositions, XPS indicates the presence of metallic Au and Cu (Figure S10). However, for 100% CuNPs, both the HRTEM-derived lattice constant and XPS analysis are consistent with the formation of a copper oxide phase (Figure S10B). Importantly, HRTEM and scanning transmission electron microscopy (STEM) analyses do not show evidence of core–shell or Janus–type particle formation and indicate that both metals are present within a single particle (*vide infra*), although they do not indicate whether the nanoparticles are homogeneous, random, or intermetallic alloys.

The elemental composition of the NPs was characterized by inductively coupled plasma mass spectrometry (ICP-MS), XPS, and STEM-energy dispersive X-ray spectroscopy (EDS) as well as PL measurements. STEM-EDS provides the spatial resolution necessary to confirm that both detected elements are located within a single particle, while ICP-MS allows us to determine the composition of the bulk colloid. EDS point spectra of individual particles indicate that the ratios of gold and copper scale roughly with the molar ratio of metal precursors added to the reactant solution. Compositions measured by ICP-MS were consistently enriched in gold relative to the initial molar ratio used for the synthesis (Table 1 and Figure S12). This apparent enrichment may be expected, as it is well known that copper leaches from NPs during extensive washing procedures.[24−27] We note that powder X-ray diffraction (XRD), a technique routinely used for the bulk characterization of larger NPs, did not provide useful composition information. The combined effects of small particle size ($d$ < 3 nm) and particle lattice strain (as evidenced by HRTEM analysis) produced Scherrer broadening that prohibited comparison between NP types.

To gain a better understanding of the elemental distribution throughout these particles, and specifically to distinguish between the formation of core–shell, Janus, or alloyed morphologies, the NPs were characterized by STEM imaging coupled with high-angle annular dark field (HAADF) and EDS. As was found from the HRTEM analysis, STEM-HAADF images are consistent with the formation of alloyed NP structures (Figures 2 and S11), and no evidence of core–shell segregation of Au and Cu can be observed. STEM-EDS point spectra taken from individual NPs indicate that gold and copper exist within a single nanostructure (Figures 2 and S11).


dx.doi.org/10.1021/ja400569u | *J. Am. Chem. Soc.* 2013, 135, 5266–5269

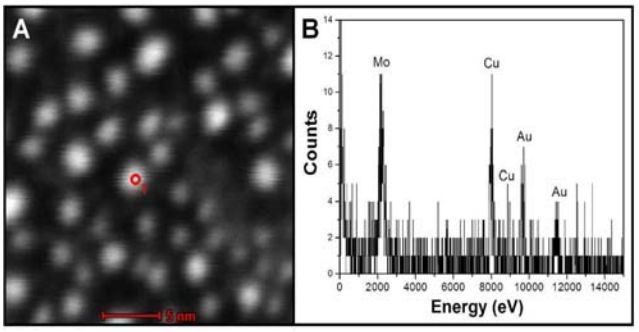


**Figure 2.** (A) STEM-HAADF image and (B) corresponding EDS spectrum demonstrating the elemental composition of a single $Au_xCu_y$NP (40:60 Au:Cu ratio). The spectrum is taken at the position indicated by the red circle; the Mo signal in the EDS spectrum originates from the molybdenum 400 mesh TEM grid used to image the particles.

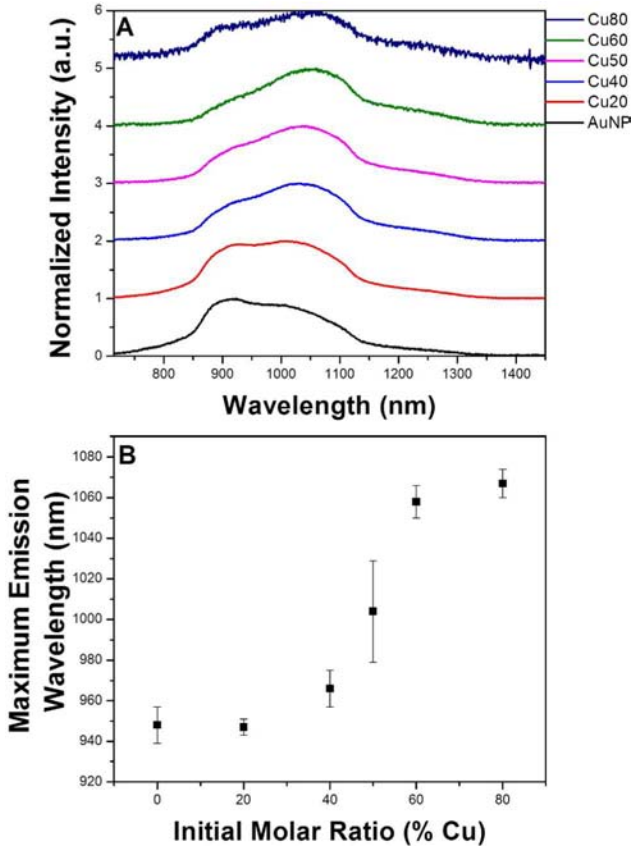


**Figure 3.** (A) Normalized and offset emission spectra of $Au_xCu_y$NPs, excitation at 360 nm. (B) Average emission wavelength as a function of the initial molar ratio of Cu.

With discrete, alloyed NPs in hand, we correlated particle architecture with PL and found a strong relationship between particle composition and particle PL properties (Figure 3). As the molar ratio of copper increases, the PL emission maximum undergoes a bathochromic shift from 947 to 1067 nm (Figure 3). Yet the full width at half-maximum (fwhm) of the peak remains similar, even though the peak shape and position change with copper content (Table 1). The source of the peak asymmetry is still under investigation and consistent with other PL reports from pure AuNPs.[2,5,6,11] However, we do not find correlation of the observed PL with a direct emission from CuNPs or copper complexes. Control experiments were performed to rule out the impact of NP concentration, aqueous copper, and physical mixtures of AuNPs and CuNPs on the observed emission shifts (Figures S13−S15). Excitation spectra were collected to determine the excitation peak maximum while monitoring the emission at 950 nm. An excitation maximum was found at approximately 360 nm for all tested compositions of $Au_xCu_y$ NPs (Figure S16). Currently, we cannot report a definitive assignment of this excitation; however, the wavelength is consistent with previously reported excitation of surface gold(I)−thiolates.[28,29]

The relative luminescence quantum yield of the NPs was evaluated by using a ytterbium complex $[Yb(tropolone)_4]^-$ as a NIR reference standard ($\Phi_r$ = 0.019 in DMSO) using optically dilute aqueous solutions (absorbance at 340 nm is < 0.2; Figure S17).[30] The calculated $\Phi$ of 100% AuNPs ($\Phi = 1.9 \times 10^{-4}$, see Table 1) is within the range of previously reported quantum yields for similar structures, which vary from $10^{-5}$ to $10^{-1}$ (determined at various emission wavelengths).[5,6] The measured $\Phi$ increases from a composition of pure gold to 25% Cu (initial molar ratio) and then decreases with additional Cu incorporation (Figure S18).

Since the PL properties of small noble metal clusters have been shown to vary with NP size (similar to semiconductor quantum dots),[7] we examined these features as a function of the particle diameter. No correlation was found between the emission peak wavelength and either the size of the metal core or hydrodynamic radius (Figure S19). Taken together, these observations are consistent with a surface-based PL excited state governed by excitation of the gold(I)−thiolate charge-transfer band[2] and further indicate that composition may be a key synthetic tool for tuning the photophysical properties of small metal NPs.

A crucial parameter in determining the utility of these NPs is their brightness ($\varepsilon \times \Phi$),[31] which must be evaluated at the optically dilute limit, and is a figure of merit to describe the probability of absorption and emission of photons for a given system.[32] Extinction coefficients were calculated using UV−vis absorbance spectra (Figures S2 and S20), the concentration of gold and copper as measured by ICP-MS (Table S2), and the average particle diameter as determined by HRTEM (Figure S3). By tuning the molar ratio of Au and Cu, we are able to produce alloyed NPs that are more than an order of magnitude brighter than the brightest lanthanide probe (3281 $M^{-1}$ $cm^{-1}$ for 60:40 Au:Cu ratio NPs vs 83 $M^{-1}$ $cm^{-1}$ for a previously reported sensitized lanthanide complex (Yb(III)TsoxMe)).[33] Interestingly, the gold-copper alloys also exhibit enhanced emission intensity (a 10−29% $\Phi$ relative enhancement, Figure S21), under biologically relevant conditions (0.020 M HEPES buffer pH of 7.2, $I$ = 0.10 M NaCl), relative to the same NPs in NANOpure water.

In summary, we have outlined a straightforward synthesis of small, discrete $Au_xCu_y$ NP alloys that display composition-tunable NIR emission. The brightness of these NPs exceeds that of the brightest ($\varepsilon \times \Phi$) NIR-emitting lanthanide probes. Fundamentally, these NP alloys provide a new platform to investigate the structural origins of small metal nanoparticle photoluminescence. Practically, the observation of these PL phenomena indicate a promising class of stable and tunable NIR probes that can be readily translated into biological settings.


dx.doi.org/10.1021/ja400569u | J. Am. Chem. Soc. 2013, 135, 5266−5269

## ■ ASSOCIATED CONTENT

### Supporting Information

Contains detailed descriptions of methods used for nanoparticle synthesis and characterization. This material is available free of charge via the Internet at http://pubs.acs.org.

## ■ AUTHOR INFORMATION


### Corresponding Author

jem210@pitt.edu


### Notes

The authors declare no competing financial interest.

## ■ ACKNOWLEDGMENTS

This work was supported by the National Science Foundation (CHE − 1253143), the Central Research Development Fund administered by the Office of Research and the University Research Council at the University of Pittsburgh and the University of Pittsburgh. We thank Dr. N. Thomas Nuhfer at Carnegie Mellon University and Dr. Dingqiang Li at Youngstown State University for generosity in using their electron microscopy facilities. We thank Prof. Sean Garrett-Roe for assistance in developing MatLab code to analyze the particle size distributions from raw $^1$H diffusion NMR data. We also thank Prof. Stephane Petoud for use of the fluorometer and related equipment.

## ■ REFERENCES


(1) Cortie, M. B.; McDonagh, A. M. *Chem. Rev.* **2011**, *111*, 3713.
(2) Zheng, J.; Zhou, C.; Yu, M.; Liu, J. *Nanoscale* **2012**, *4*, 4073.
(3) Zheng, J.; Nicovich, P. R.; Dickson, R. M. *Annu. Rev. Phys. Chem.* **2007**, *58*, 409.
(4) Fang, Y.; Chang, W.-S.; Willingham, B.; Swanglap, P.; Dominguez-Medina, S.; Link, S. *ACS Nano* **2012**, *6*, 7177.
(5) Huang, T.; Murray, R. W. *J. Phys. Chem. B* **2001**, *105*, 12498.
(6) Link, S.; Beeby, A.; FitzGerald, S.; El-Sayed, M. A.; Schaaff, T. G.; Whetten, R. L. *J. Phys. Chem. B* **2002**, *106*, 3410.
(7) Zheng, J.; Zhang, C.; Dickson, R. M. *Phys. Rev. Lett.* **2004**, *93*, 077402.
(8) Zhou, C.; Sun, C.; Yu, M.; Qin, Y.; Wang, J.; Kim, M.; Zheng, J. *J. Chem. Phys.* **2010**, *114*, 7727.
(9) Dulkeith, E.; Niedereichholz, T.; Klar, T. A.; Feldmann, J.; von Plessen, G.; Gittins, D. I.; Mayya, K. S.; Caruso, F. *Phys. Rev. B: Condens. Matter Mater. Phys.* **2004**, *70*, 205424.
(10) Tcherniak, A.; Dominguez-Medina, S.; Chang, W.-S.; Swanglap, P.; Slaughter, L. S.; Landes, C. F.; Link, S. *J. Phys. Chem. C* **2011**, *115*, 15938.
(11) Huang, T.; Murray, R. W. *J. Phys. Chem. B* **2003**, *107*, 7434.
(12) Wang, G. G., R.; Kalyuzhny, G.; Choi, J.-P.; Murray, R. W. *J. Phys. Chem. B* **2006**, 110.
(13) Parker, J. F.; Fields-Zinna, C. A.; Murray, R. W. *Acc. Chem. Res.* **2010**, 43.
(14) Ruban, A. V.; Skriver, H. L.; Norskov, J. K. *Phys. Rev. B* **1999**, *59*, 15990.
(15) Nilekar, A. U.; Ruban, A. V.; Mavrikakis, M. *Surf. Sci.* **2009**, *603*, 91.
(16) Hume-Rothery, W.; Powell, H. M. *Z. Kristallogr.* **1935**, 91.
(17) Schaak, R. E.; Sra, A. K.; Leonard, B. M.; Cable, R. E.; Bauer, J. C.; Han, Y. F.; Means, J.; Teizer, W.; Vasquez, Y.; Funck, E. S. *J. Am. Chem. Soc.* **2005**, *127*, 3506.
(18) Sra, A. K.; Ewers, T. D.; Schaak, R. E. *Chem. Mater.* **2005**, *17*, 758.
(19) Bondi, J. F.; Misra, R.; Ke, X. L.; Sines, I. T.; Schiffer, P.; Schaak, R. E. *Chem. Mater.* **2010**, *22*, 3988.
(20) Udayabhaskararao, T.; Sun, Y.; Goswami, N.; Pal, S. K.; Balasubramanian, K.; Pradeep, T. *Angew. Chem., Int. Ed.* **2012**, *51*, 2155.
(21) Crespo, O.; Gimeno, M. C.; Laguna, A.; Larraz, C.; Villacampa, M. D. *Chem.—Eur. J.* **2007**, *13*, 235.
(22) Crespo, O.; Gimeno, M. C.; Laguna, A.; Lahoz, F. J.; Larraz, C. *Inorg. Chem.* **2011**, *50*, 9533.
(23) Okamoto, H.; Chakrabarti, D. J.; Laughlin, D. E.; Massalski, T. B. *Bull. Alloy Phase Diagr.* **1987**, *8*, 454.
(24) Motl, N. E.; Ewusi-Annan, E.; Sines, I. T.; Jensen, L.; Schaak, R. E. *J. Phys. Chem. C* **2010**, *114*, 19263.
(25) Oezaslan, M.; Heggen, M.; Strasser, P. *J. Am. Chem. Soc.* **2011**, *134*, 514.
(26) Pachón, L. D.; Rothenberg, G. *Appl. Organomet. Chem.* **2008**, *22*, 288.
(27) Mayrhofer, K. J. J.; Hartl, K.; Juhart, V.; Arenz, M. *J. Am. Chem. Soc.* **2009**, *131*, 16348.
(28) Zhu, M.; Aikens, C. M.; Hollander, F. J.; Schatz, G. C.; Jin, R. *J. Am. Chem. Soc.* **2008**, *130*, 5883.
(29) Devadas, M. S.; Kim, J.; Sinn, E.; Lee, D.; Goodson, T.; Ramakrishna, G. *J. Phys. Chem. C* **2010**, *114*, 22417.
(30) Zhang, J.; Badger, P. D.; Geib, S. J.; Petoud, S. *Angew. Chem., Int. Ed.* **2005**, *44*, 2508.
(31) McNaught, A. D.; Wilkinson, A.; Nic, M.; Jira, J.; Kosata, B. In *IUPAC Compendium of Chemical Terminology* (the "Gold Book"), 2nd ed.; Blackwell Scientific Publications: Oxford, 1997.
(32) Werts, M. H. V. In *Lanthanide Luminescence*; Hänninen, P., Härmä, H., Eds.; Springer: Berlin Heidelberg, 2011; Vol. 7, p 133.
(33) Comby, S.; Imbert, D.; Chauvin, A. S.; Bunzli, J. C. G. *Inorg. Chem.* **2006**, *45*, 732.